Electronic Supplementary Material (ESI) for New Journal of Chemistry.

Supporting Information

Processable soft conducting fibers of self-assembled (2,5-diphenyl-2H-1,2,3-triazole-4-carbonyl)-L-phenylalaninate

Sahabaj Mondal,[a] Olamilekan Joseph Ibukun,[a] Milan Gumtya[a] and Debasish Haldar*[a]

[a] Department of Chemical Sciences, Indian Institute of Science Education and Research Kolkata, Mohanpur 741246, West Bengal, India

Corresponding Author

Debasish Haldar − Email: deba_h76@yahoo.com, deba_h76@iiserkol.ac.in

Table of contents

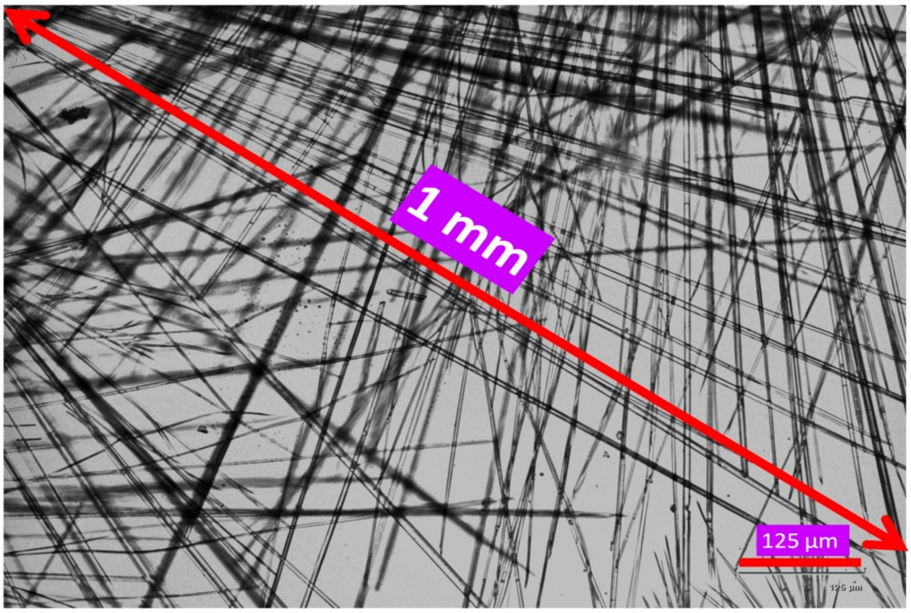
1 mm
125 µm
125 µm

Figure S1. (a) Fluorescence microscopy image of self-assembled peptide ultralong microtubes formed by an evaporation process.

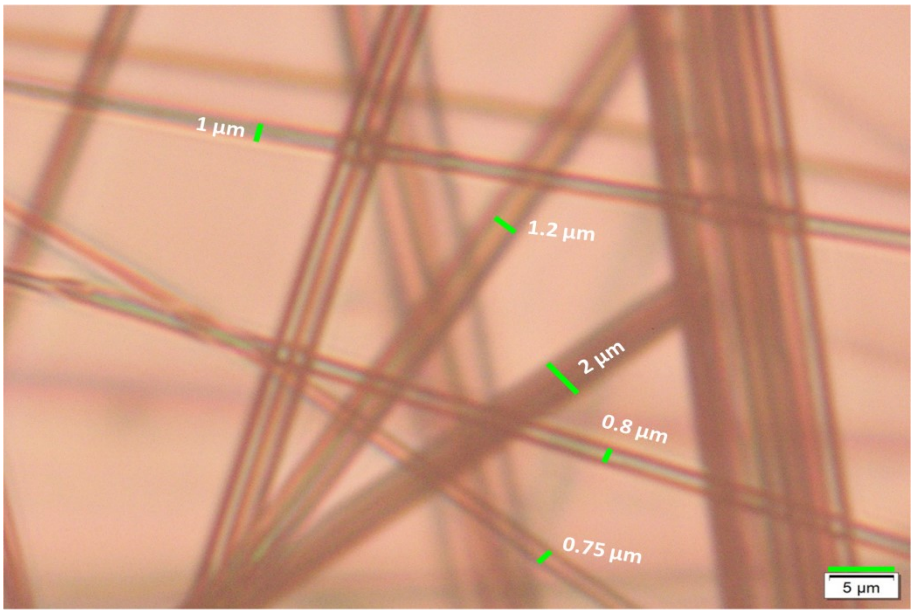

Figure S2. (a) POM image of self-assembled peptide ultralong microtubes formed by an evaporation process.

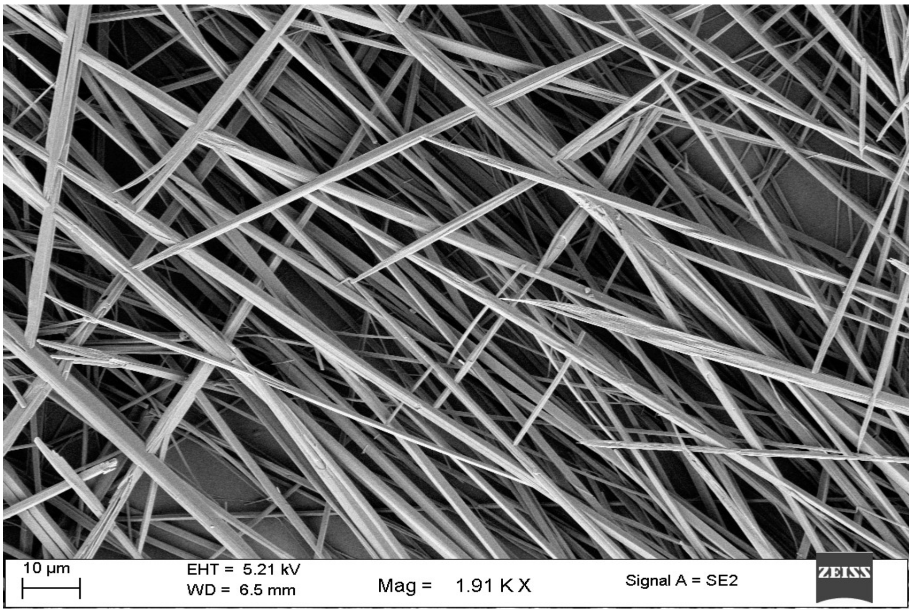

Figure S3. (a) SEM images of self-assembled peptide ultralong microtubes formed by an evaporation process.

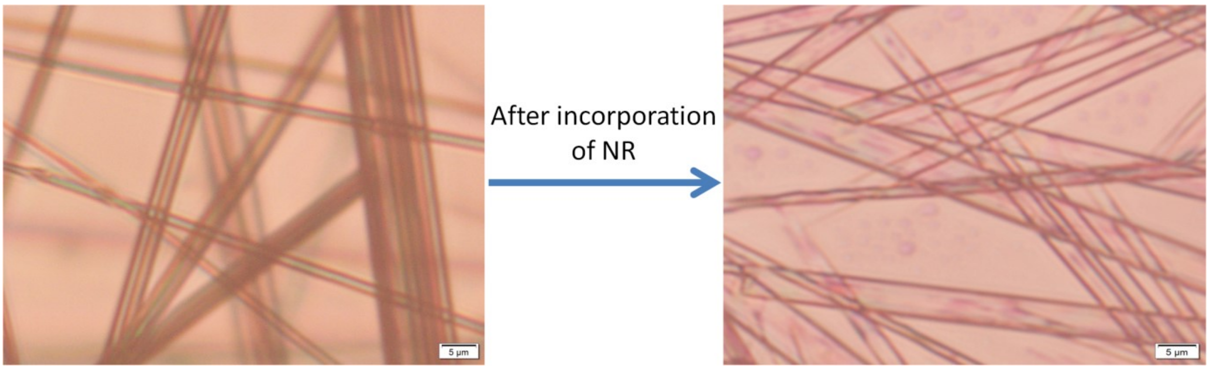

Figure S4: Images show the change after the incorporation of NR.

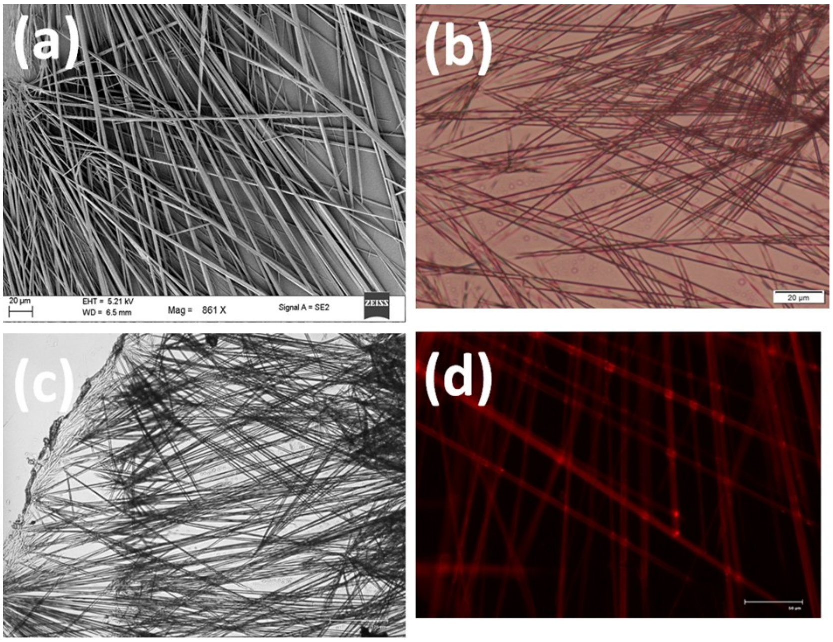

Figure S5. (a) SEM image and (b) POM image, (c) bright-field image, and (d) confocal image of Nile Red-incorporated peptide microtubes as obtained from acetonitrile.

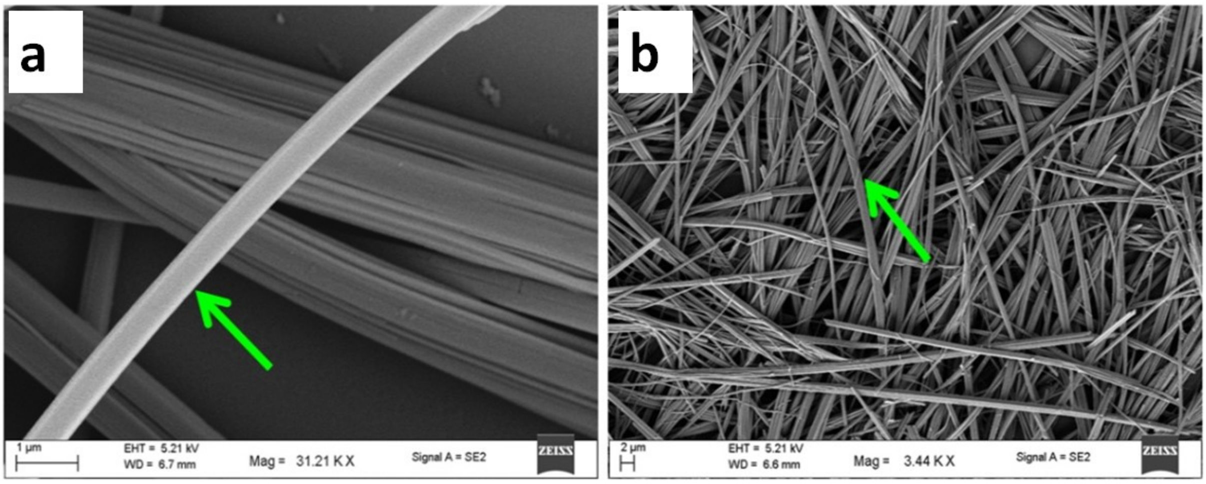

Figure S6. The shape of the self-assembling structure can significantly affect conductivity. Long, straight microtubes are the most conductive, while shorter or curved assemblies have higher resistance. SEM images of the microstructures obtained from different experimental conditions; (a) ethanol, and (b) ethanol/water.

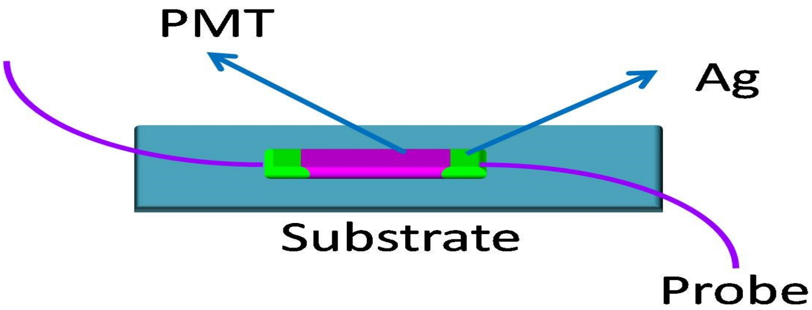

Figure S7: Schematic of the semiconducting measurement setup. Here PMT denotes peptide microtube.

Solvent	Voltage (V)	Current (nA)	Conductance (nS)	Bnadgap energy (eV) (Tauc plot)
Acetonitrile	0.2	22.03	100.2	3.71
Ethanol	0.2	8.2	41	3.73
Acetonitrile/ water (1 : 1)	0.2	28.5	142.5	3.70
Ethanol/water (1 : 1)	0.2	4.4	22	3.76

Table S1: Electrical output data of different microstructures obtained during semiconductivity measurements.

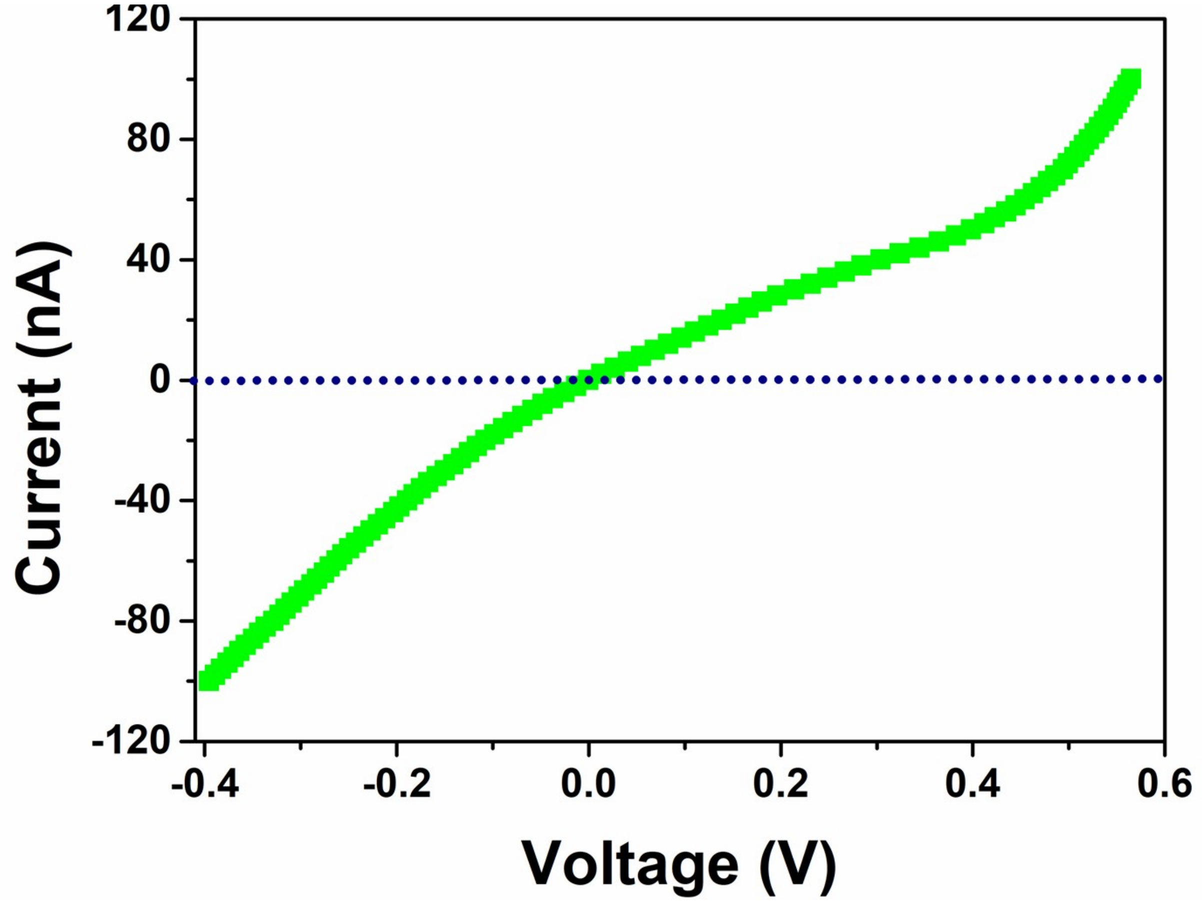

Figure S8: I-V curve of microtube obtained from ACN/water.

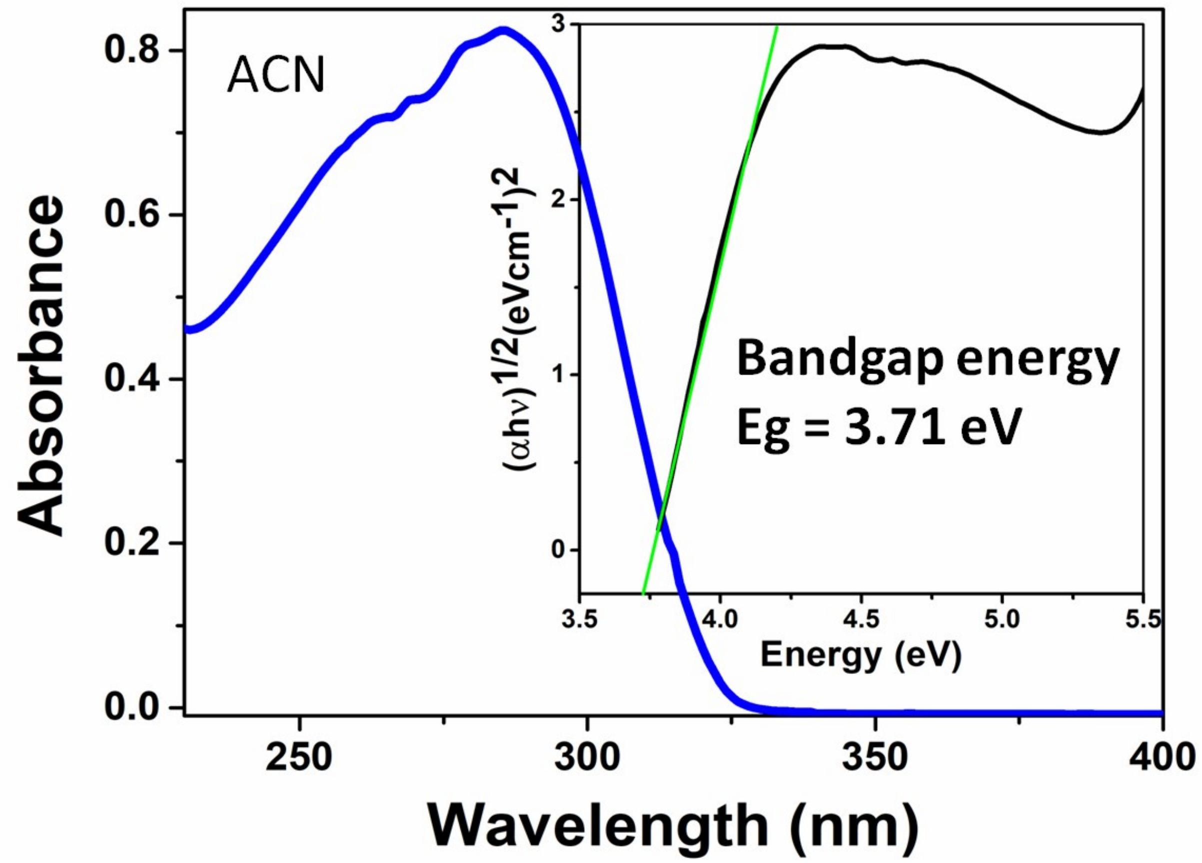

Figure S9: Tauc plot to calculate band gap of hexagonal microtube as obtained from ACN solvent.

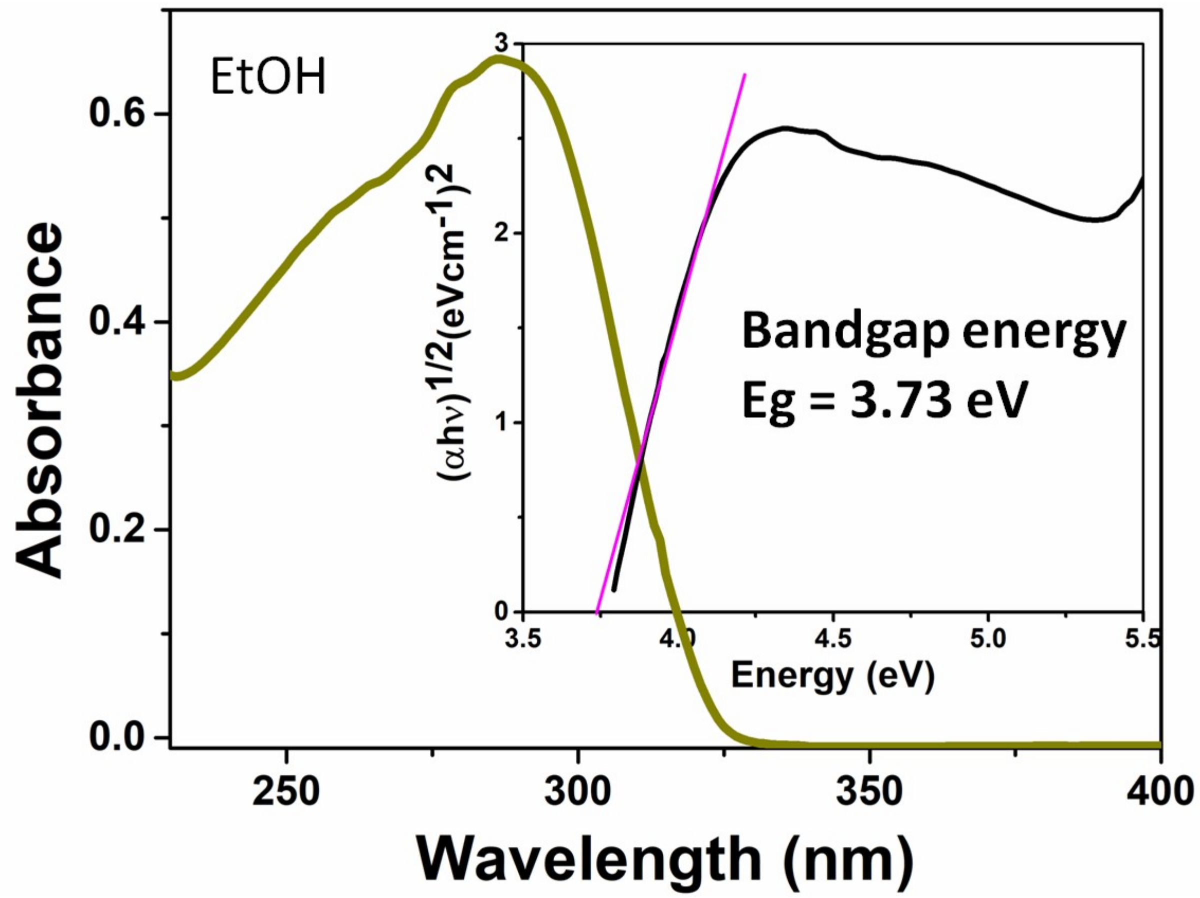

Figure S10: Tauc plot to calculate the band gap of microfiber as obtained from ethanol.

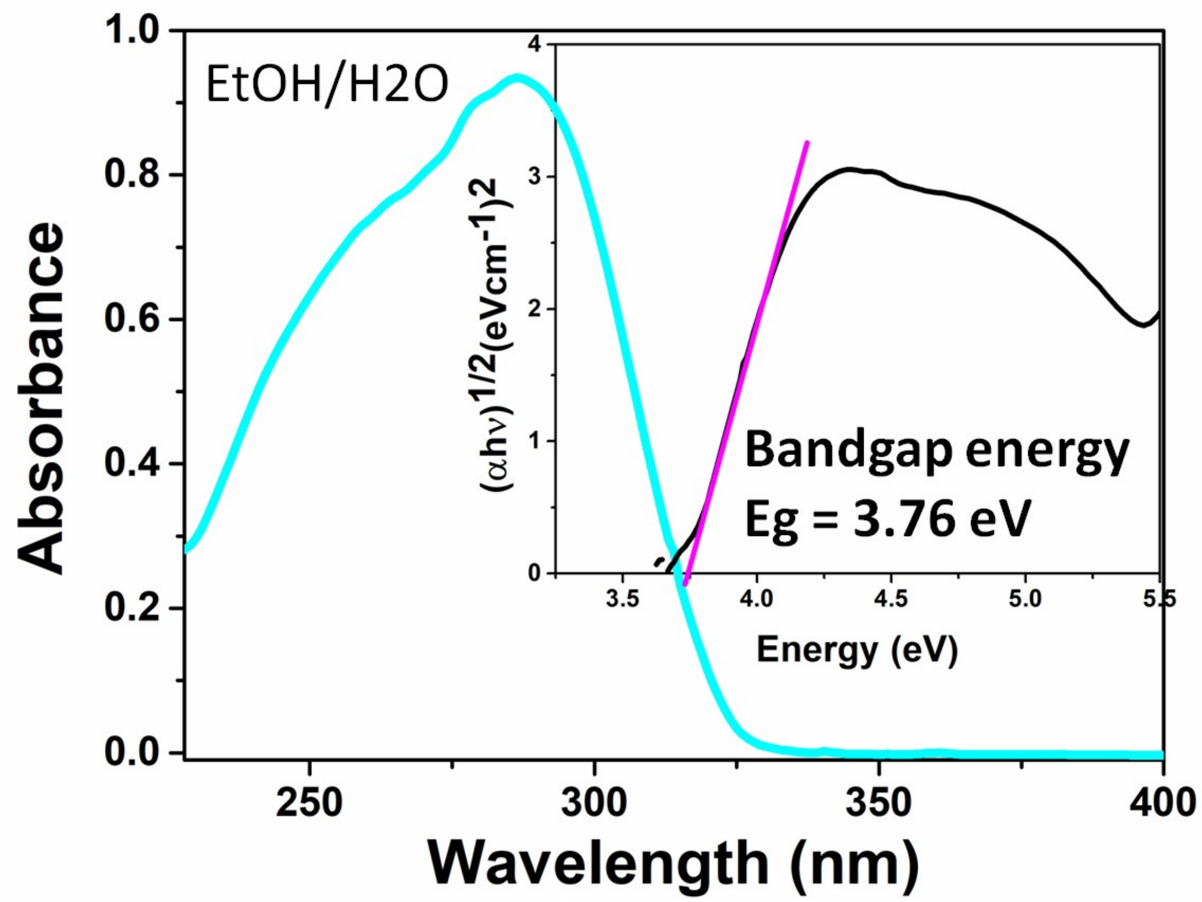

Figure S11: Tauc plot to calculate band gap of microfiber as obtained from ethanol/H_2O mixture.

Sample preparation: Solutions of compound 1 (4.7 mM) were prepared by dissolving samples in ACN and EtOH, followed by equilibration for 30 min. For the ACN/water and EtOH/water solution, first compound 1 (9.4 mM) solutions were prepared by dissolving samples in ACN and EtOH, then diluted to 4.7 mM, followed by equilibration for 30 min.

Fourier-Transform Infrared Spectroscopy

Sample aliquots were taken as a droplet on the surface of the ATR cell (Platinum ATR) of an IR spectrometer (Bruker, model no: Alpha) to obtain IR spectra). The background spectra were subtracted from each sample spectrum. The spectra were recorded at room temperature.

Polarized optical microscopy (POM)

POM images determined the morphologies of the compounds. A tiny amount of the sample was drop-cast on a glass slide and then dried by evaporation and was visualized at 40× or 100× magnification on an Olympus optical microscope equipped with a polarizer and CCD camera.

Field emission scanning electron microscopy

SEM samples were prepared following a drop-casting method. Briefly, samples were drop-cast on a glass coverslip and dried under a vacuum before imaging. The images were captured using a gold coating using an FE-SEM apparatus (JEOL Scanning Microscope-JSM-6700F).

Fluorescence Microscopy

Both peptide and Nile red (NR) dye-containing solution was drop cast on a glass slide. The images were captured upon excitation at 590 nm.

Absorption spectroscopy

The absorption spectra of the samples were measured on a Perkin Elmer UV/Vis spectrometer (Lambda35) using a quartz cell with a 1 cm path length.

Fluorescence spectroscopy

All fluorescence spectra were recorded on a Perkin Elmer fluorescence spectrometer (L.S. 55) using a 1 cm path-length quartz cell. Slit widths of 2.5 nm/2.5nm were used.

Powder X-ray diffraction:

The powder XRD measurements were performed with a Rigaku (mini flex II, Japan) powder X-ray diffractometer having Cu Kα = 1.54059 Å radiation. Powder samples were obtained from the respective solution. The slow evaporation method was used to get a powder sample for x-ray diffraction. The dried pieces were then placed in a zero-background holder, and the spectra were obtained by fixing up the scanning window.

Transmission Electron Microscopy.

The TEM studies were performed using a small amount of the ACN solution of the compound on a carbon-coated copper grids (300 mesh) by slow evaporation and allowed to dry under vacuum at 30°C for 2 days. A drop of uranil acetate solution (freshly prepared 2% uranil acetate solution) was added and dried under vacuum for 10 h. Images were taken in both the transmission mode. TEM was done by a JEOL JEM 2010 electron microscope.

Electrical characterization

Chip configuration. Electrical characterizations were conducted using a prefabricated chip with silver electrodes (Figure S7). The chip configuration consists of a silicon wafer with a top silicon oxide layer. Silver electrodes were deposited on top of the wafer using an adhesion layer. Chips were fabricated at the Indian Institute of Science Education and Research, Kolkata, India. Figure S7: General scheme of a chip we used for the electrical measurements.

Determine the Band Gap Energy of the Modified Semiconductor Based on UV−Vis Spectra

The band gap energy of a semiconductor describes the energy needed to excite an electron from the valence band to the conduction band. Accurately determining the band gap energy is crucial in predicting semiconductors' photophysical and photochemical properties. In particular, this parameter is often referred to when the photocatalytic properties of semiconductors are discussed. In 1966 Tauc proposed a method of estimating the band gap energy of amorphous semiconductors using optical absorption spectra.[1] His proposal was further developed by Davis and Mott.[2,3] The Tauc method is based on the assumption that the energy-dependent absorption coefficient α can be expressed by the following equation (1):

$$(\alpha . h\upsilon)^{1/\gamma} = \mathrm{B}(h\upsilon - \mathrm{E_g}) \qquad (1)$$

where h is the Planck constant, v is the photon's frequency, $\mathrm{E_g}$ is the band gap energy, and B is a constant. The γ factor depends on the nature of the electron transition and is equal to 1/2 or 2 for the direct and indirect transition band gaps, respectively.[4]

The region showing a steep, linear increase of light absorption with increasing energy is characteristic of semiconductor materials. The x-axis intersection point of the linear fit of the Tauc plot gives an estimate of the band gap energy.[5]

Computational Studies

We carried out geometry optimizations and vibrational frequency analyses without any symmetry constraints at the level of density functional theory (DFT) methods in Gaussian 09. We used Beck's three-parameter hybrid exchange functional,[6,7] combined with the Lee–

Yang–Parr nonlocal correlation function (abbreviated as B3LYP).[8] The split-valence basis set with diffuse functions, 6-311(d), was employed for all atoms. Vibrational frequencies were calculated to verify that no negative frequency was present in the optimized structures.

General Information:

Reactions were performed under air using oven-dried glassware. MeCN and other solvents were purchased from Merck Life Science Private Limited and were directly used without further drying or purification. All reagents were obtained from commercial sources and used without further purification. Thin-layer chromatography was performed on Merck pre-coated silica gel 60 F254 aluminum sheets with detection under UV light at 254 nm. Chromatographic separations were carried out on chempure silica gel (100−200 mesh). Nuclear magnetic resonance (NMR) spectroscopy was performed using JEOL 400 MHz and Bruker 500 MHz spectrometers. If not otherwise specified, chemical shifts (δ) are provided in ppm.

Synthetic scheme:

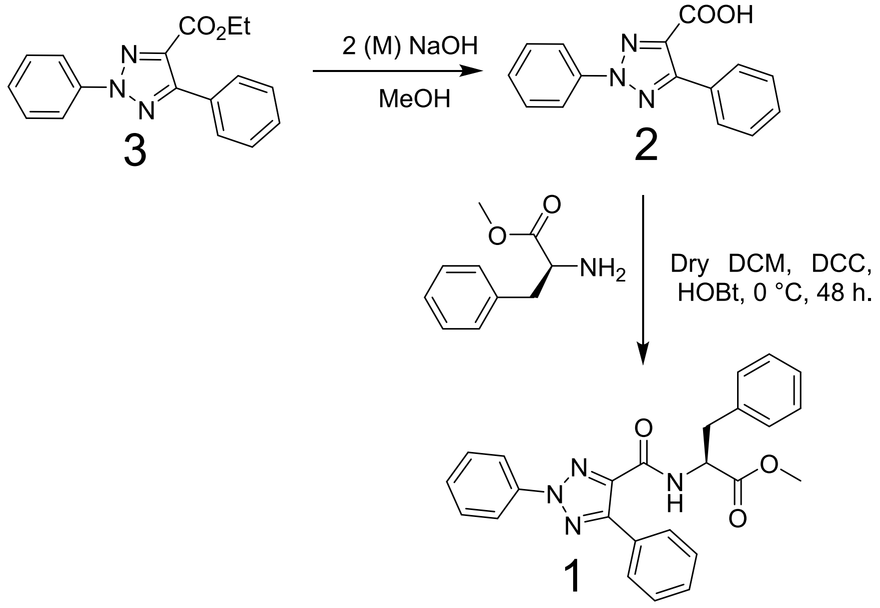

General Procedure for the Preparation of 2,5-diphenyl-2H-1,2,3-triazole-4-

carboxylic acid 2:

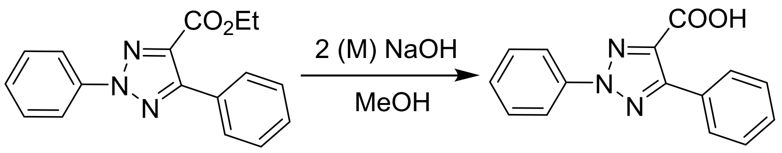

2,5-diphenyl-2H-1,2,3-triazole-4-carboxylic acid 2: To 1.485 g (5 mmol) of ethyl 2,5-diphenyl-2H-1,2,3-triazole-4-carboxylate (3), 25 mL MeOH and 2M 15 mL NaOH were added and the progress of saponification was monitored by thin layer chromatography (TLC). The reaction mixture was stirred. After 10 h, methanol was removed under a vacuum; the residue was dissolved in 50 mL of water and washed with diethyl ether (2 X 50 mL). Then the pH of the aqueous layer was adjusted to 2 using 1M HCl, and it was extracted with ethyl acetate (3 X 50 mL). The extracts were pooled, dried over anhydrous sodium sulfate, and evaporated under a vacuum. The obtained product was used directly for the next step without further purification. Yield: 1.23 g (4.6 mmol, 91.7 %).

General Procedure for the Preparation of methyl (2,5-diphenyl-2H-1,2,3-triazole-4-carbonyl)-L-phenylalaninate 1:

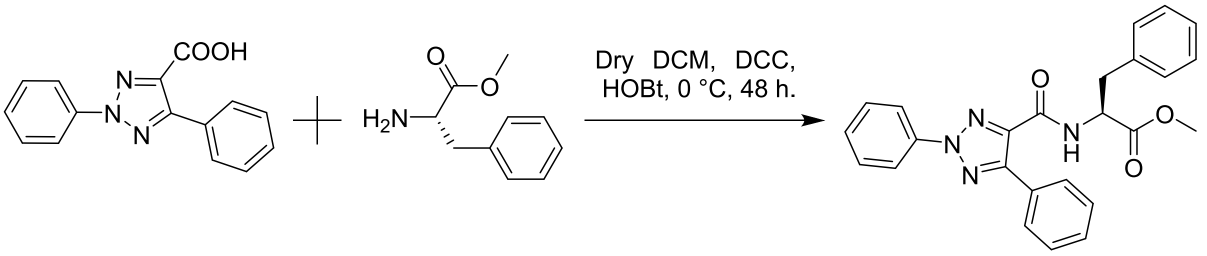

Methyl (2,5-diphenyl-2H-1,2,3-triazole-4-carbonyl)-L-phenylalaninate(F): 1.20 g (4.5 mmol) of 2,5-diphenyl-2H-1,2,3-triazole-4-carboxylic acid (2) was dissolved in 25 mL DCM in an ice-water bath. H-Phe-OMe was isolated from 1.07 g (5 mmol) of the corresponding salt of methyl ester hydrochloride by neutralization and subsequent extraction with ethyl acetate and solvent evaporation. It was then added to the reaction mixture, followed immediately by 1.03 g (5 mmol) dicyclohexylcarbodiimide (DCC) and 0.675 g (5 mmol) of HOBt. The reaction mixture was allowed to come to room temperature and stirred for 48 h. DCM was evaporated, the residue was dissolved in ethyl acetate (60 mL), and dicyclohexylurea (DCU) was filtered off. The organic layer was washed with 2M HCl (3 x 50 mL), brine (2 x 50 mL), 1M sodium carbonate (3 x50 mL), and brine (2 x50 mL) and dried over anhydrous sodium sulfate. It was evaporated in a vacuum to yield ethyl (2,5-diphenyl-2H-1,2,3-triazole-4-carbonyl)-L-phenylalaninate and purified by silica gel column (60-120 mesh size) with ethyl acetate and hexane as the eluent. Yield 1.27 g (2.9 mmol, 65.8%).

^{1}H NMR (400 MHz, $CDCl_3$) δ 8.13 (d, *J* = 7.7 Hz, 2H), 8.07 (dd, *J* = 7.9, 1.7 Hz, 2H), 7.53 (t, *J* = 7.9 Hz, 2H), 7.47 – 7.39 (m, 5H), 7.31 (d, *J* = 7.4 Hz, 2H), 7.21 (d, *J* = 1.6 Hz, 1H), 7.19 (s, 1H), 5.09 (dt, *J* = 8.0, 6.0 Hz, 1H), 3.76 (s, 3H), 3.26 (dd, *J* = 9.3, 6.0 Hz, 2H).**^{13}C NMR** (125 MHz, $CDCl_3$) δ 171.69, 159.87, 149.28, 139.02, 138.65, 135.71, 129.29, 129.28, 129.26, 129.13, 128.55, 128.32, 128.14, 127.13, 119.12, 53.08, 52.33, 38.07.

Mass spectral data TOF-MS m/z: [M+H]+ = 427.1765 , [M+Na]+ = 449.1584, [M+K]+ = 465.3715; [2M+Na]+ = 875.3274; Mcal =426.17.

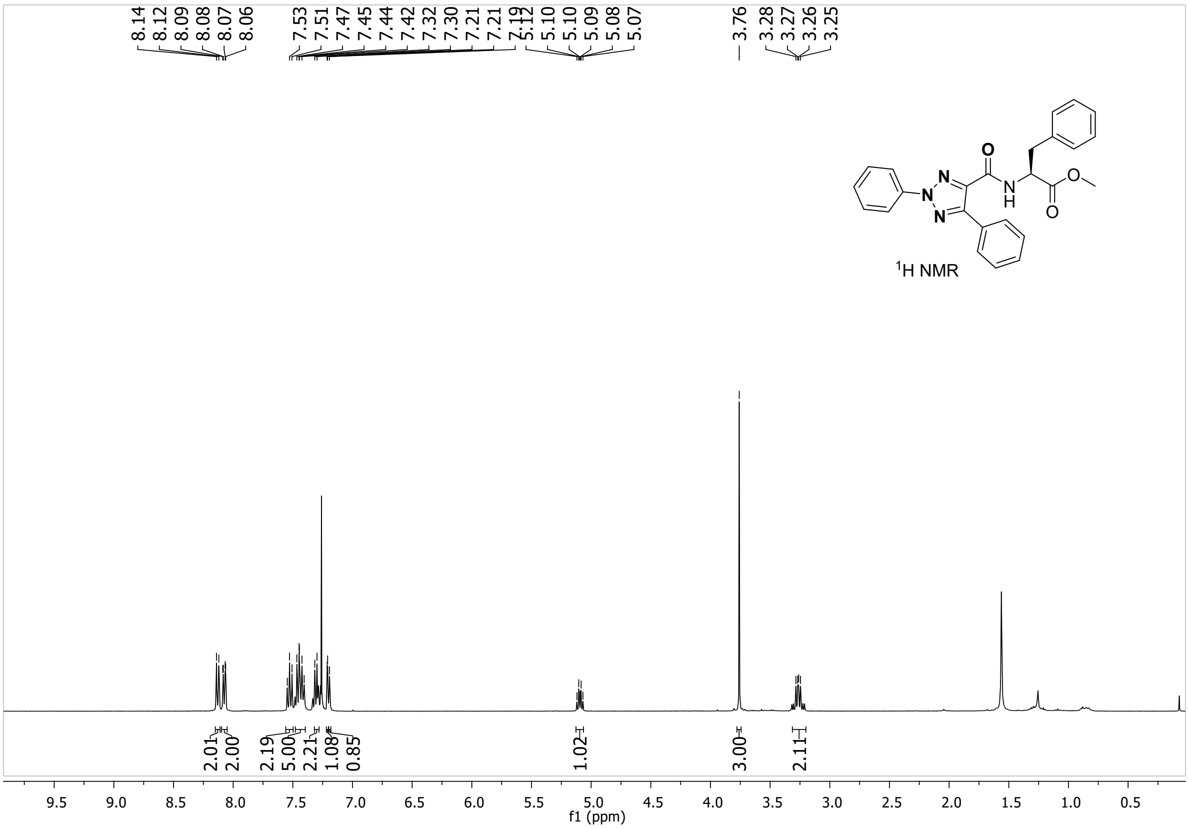

Figure S12: ^{1}H NMR (400 MHz, $CDCl_3$) of compound **1**.

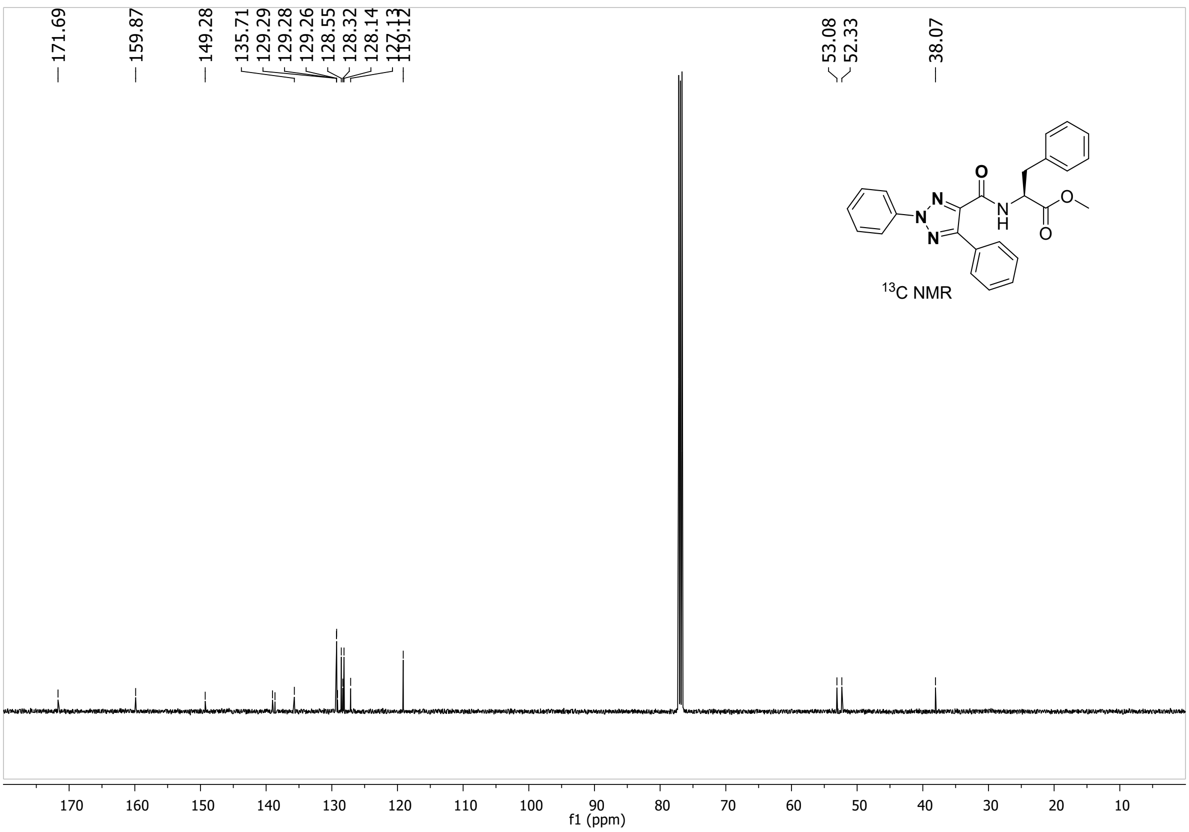

Figure S13: ^{13}C NMR (125 MHz, $CDCl_3$) of compound **1**.

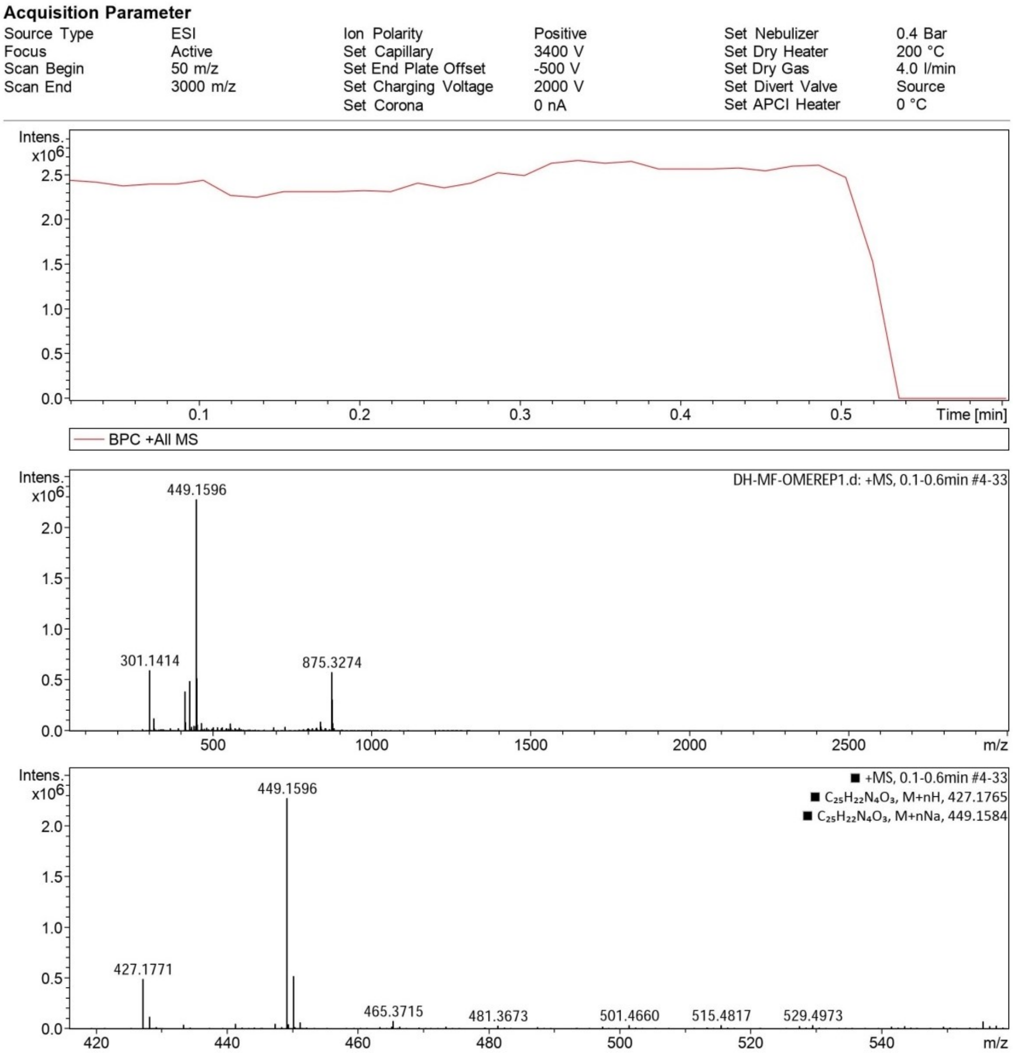

```
Acquisition Parameter
Source Type     ESI         Ion Polarity           Positive    Set Nebulizer     0.4 Bar
Focus           Active      Set Capillary          3400 V      Set Dry Heater    200 °C
Scan Begin      50 m/z      Set End Plate Offset   -500 V      Set Dry Gas       4.0 l/min
Scan End        3000 m/z    Set Charging Voltage   2000 V      Set Divert Valve  Source
                            Set Corona             0 nA        Set APCI Heater   0 °C
```

Figure S14: Mass spectrometry analysis of compound **1**.

Reference

1. Tauc, J.; Grigorovici, R.; Vancu, A. Optical Properties and Electronic Structure of Amorphous Germanium. *Phys. Status Solidi B* **1966**, *15*, 627−637.
2. Davis, E.; Mott, N. Conduction in non-crystalline systems V. Conductivity, optical absorption and photoconductivity in amorphous semiconductors. *Philos. Mag.* **1970**, *22*, 0903−0922.
3. Mott, N. F.; Davis, E. A. Electronic Processes in Non-Crystalline Materials; *OUP Oxford*, **2012**.
4. Pankove, J. I. Optical Processes in Semiconductors; *Courier Corporation*, **1971**.
5. Makuła, P.; Pacia, M.; and Macyk, W. How To Correctly Determine the Band Gap Energy of Modified Semiconductor Photocatalysts Based on UV−Vis Spectra. *J. of Phys. Chem. Lett.,* **2018,** *9*, 6814-6817.
6. Frisch, M. J.; Trucks, G. W.; Schlegel, B. H.; Scuseria, G. E.; Robb, M. A.; Cheeseman, J. R.; Scalmani, G.; Barone, V.; Mennucci, B.; Petersson, G. A.; et al. Gaussian 09, Revision D.01; *Gaussian, Inc: Wallingford, CT*, **2009**.

7. Becke, A. D. Density-functional exchange-energy approximation with correct asymptotic behavior. *Phys. Rev. A: At., Mol., Opt. Phys.* **1988**, *38*, 3098−3100.
8. Lee, C.; Yang, W.; Parr, R. G. Development of the Colic-Salvetti correlation-energy formula into a functional of the electron density. *Phys. Rev. B: Condens. Matter Mater. Phys.* **1988**, *37*, 785−789.